

Original Papers

phys. stat. sol. (a) **81**, 47 (1984)

Subject classification: 1.6 and 2; 10.2; 22.1.2

I. V. Kurchatov Institute of Atomic Energy, Moscow¹ (a)
and A. V. Shubnikov Institute of Crystallography,
Academy of Sciences of the USSR, Moscow² (b)

X-Ray Diffraction under Specular Reflection Conditions on Crystals with an Amorphous Surface Film

By

P. A. ALEKSANDROV (a), A. M. AFANASIEV (a), M. K. MELKONYAN (b),
and S. A. STEPANOV (b)

X-ray diffraction under specular reflection conditions is theoretically studied on a crystal with a surface amorphous film. It is shown that by choosing various values of the incident angle it is possible to detect surface amorphous films of various thickness from few nanometers and greater. The discussions are confirmed with calculations of rocking curves for the case of silicon single crystals with surface amorphous films of various thickness (CuK α radiation, 220 reflection). The results can be applied also for crystalline films with lattice spacings distinguished from the substrate ones by a value as small as $\approx 10^{-4}$ or greater.

Теоретически исследована дифракция рентгеновских лучей в условиях полного внешнего отражения на кристалле с поверхностной аморфной пленкой. Показано, что выбирая различные углы падения, можно определять аморфные пленки различной толщины, от десятков ангстрем и более. Обсуждение иллюстрируется расчетами для случая монокристалла кремния с поверхностными аморфными пленками различной толщины (CuK α излучение, 220 отражение). Результаты могут быть применимы также к кристаллическим пленкам с параметром решетки, отличным от параметра решетки подложки на величину $\approx 10^{-4}$ или более.

1. Introduction

In recent years significant progress in extending the possibilities of crystal structure studies using X-ray diffraction has taken place. One such type of studies has been reported in [1], in which an essentially new diffraction scheme, called "parallel Bragg diffraction" has been demonstrated. An X-ray beam is directed into the crystal at a small glancing angle of incidence and simultaneously the conditions of Laue case diffraction for the planes normal to the surface are met (see Fig. 1). The small value of the incident angle provides a strong specular reflection of both incident and diffracted waves from the crystal surface and, in principle, it gives the possibility to study the crystalline structure of thin films over the depth, being as small as a few nanometers or greater. In [1] an excellent example of crystal structure analysis of aluminium films grown on GaAs monocrystal was given. In the next paper of the same authors the reconstruction of a Ge crystal surface has been investigated using synchrotron radiation [2]. But having shown the possibilities of the method the authors pointed out rather great difficulties of this technique connected with the necessity of X-ray beam collimation in two mutually perpendicular planes: in the vertical plane (because of the glancing angle of incidence) and in a horizontal plane (in order to realize the diffraction conditions). Effectively this method could be used only for

¹) 123182 Moscow, USSR.

²) Leninskii prospekt 59, 117333 Moscow, USSR.

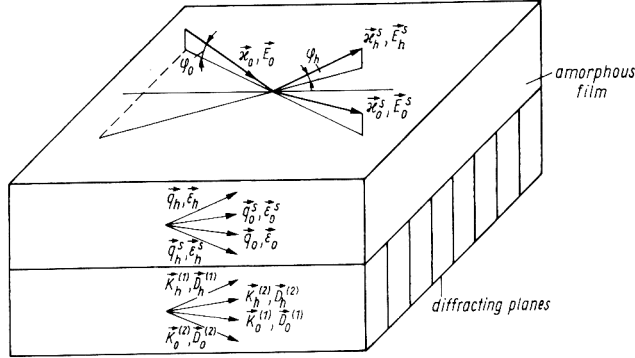


Fig. 1. The scheme of diffraction scattering of X-rays under specular reflection conditions from a crystal with an amorphous surface film

crystals with a subsurface layer having a lattice parameter strongly different from that of the substrate. In this case it will be sufficient to provide a rather rough horizontal collimation of the incident beam, the angle of divergence being of the same order as the angular separation between diffraction maxima from layer and substrate, respectively. But for small differences between the lattice parameters of the layer and the substrate this technique appeared to be practically useless.

As shown in [3] the parallel Bragg-diffraction scheme has a wider range of applications. This fact is connected with the following physical effect which was not noted by previous authors having investigated this problem [1, 2, 4 to 6]. The whole point is that the value of the exit angle φ_h of the specularly reflected-diffracted wave (\vec{x}_h^s wave in Fig. 1) depends on how exactly the Bragg condition is satisfied. In other words, there is a rigid relation between the values of the angles φ_0 and φ_h and the value of the parameter α determining the deviation from the exact Bragg condition,

$$\varphi_0^2 = \varphi_h^2 + \alpha. \quad (1)$$

Due to the small value of the angle φ_h , a very slight variation of the parameter α causes a strong variation of the angle φ_h (φ_0 being constant),

$$\delta\varphi_h = -\frac{\delta\alpha}{2\varphi_h}. \quad (2)$$

Variation of the α -value $\delta\alpha \approx 0.1''$ causes $\delta\varphi_h \approx 1'$, i.e. the angular scale increases by several orders of magnitude. It is this fact which enables one to carry out a principally new experimental scheme in which it is possible to refrain completely from collimation through α and to carry out measurements of the reflected-diffracted intensity distribution over the value of the angle φ_h . In this technique one always measures the intensity with variations of angles φ_0 and φ_h as large as minutes of arc and, on the other hand, the curves obtained will show very slight deviations of subsurface lattice spacing corresponding to deviations in α as small as fractions of a second of arc. Evidently the absence of collimation through α makes the experimental realization simple and it seems that the technique in the proposed version will have a wide range of practical applications.

Recently such a scheme has been experimentally realized in [7]. In this paper the fundamental results of the theoretical analysis [3] of X-ray diffraction under specular reflection conditions for ideal crystals have been experimentally confirmed.

Naturally it is of essential interest to consider the effect of various defects in the subsurface layer on the diffraction pattern. The present paper deals with the analysis of this diffraction scheme in the case where a thin amorphous film occurs on a perfect crystal surface. It will be shown below that films with thickness from 1 to 100 nm are revealed in the diffraction curves if a suitable value of the incident angle is chosen.

2. General Expression for the Intensity of the Reflected-Diffracted Wave

Let us consider a crystal with an amorphous surface film of thickness t . We take the plane wave to be incident on the crystal surface following the geometry shown by Fig. 1. As in the case of a crystal without a film [3], the X-ray wave field above the entrance surface consists of three waves,

$$\mathbf{E}(\mathbf{r}) = \mathbf{E}_0 e^{i\boldsymbol{\kappa}_0 \cdot \mathbf{r}} + \mathbf{E}_0^s e^{i\boldsymbol{\kappa}_0^s \cdot \mathbf{r}} + \mathbf{E}_h^s e^{i\boldsymbol{\kappa}_h^s \cdot \mathbf{r}}. \quad (3)$$

Here and below the notations of [3] will be used.

In the amorphous film one has a set of transmitted and diffracted waves in the directions of both incident and diffracted waves, respectively,

$$\mathbf{E}_0^{\text{am}}(\mathbf{r}) = \sum_{j=0,h} \mathbf{E}_j e^{i\boldsymbol{\kappa}_j \cdot \mathbf{r} + i\boldsymbol{\kappa}_j^{\text{am}} z} + \mathbf{E}_j^s e^{i\boldsymbol{\kappa}_j \cdot \mathbf{r} - i\boldsymbol{\kappa}_j^{\text{am}} z} \quad (4)$$

where the following notations are used:

$$y_{0,h}^{\text{am}} = \sqrt{\varphi_{0,h}^2 + \chi_0^{\text{am}}}, \quad (5)$$

χ_0^{am} being the Fourier component of the susceptibility of the film, z the coordinate along the internal surface normal, \mathbf{E} a coordinate vector along the surface.

Inside the crystal (which is considered to be infinitely thick) the field consists of transmitted and diffracted waves,

$$\mathbf{D}(\mathbf{r}) = \sum_{j=1}^2 \mathbf{D}_0^{(j)} e^{i\boldsymbol{\kappa}_0 \cdot \mathbf{r} + iu^{(j)}z} + \mathbf{D}_h^{(j)} e^{i\boldsymbol{\kappa}_h \cdot \mathbf{r} + iu^{(j)}z}. \quad (6)$$

The values $u^{(j)}$ and the relationship between the amplitudes $D_0^{(j)}$ and $D_h^{(j)}$ are determined from the fundamental equations of the dynamical theory which have been written for σ -polarized waves in [3] (I.7). In what follows the formulae of [3] will be referred to with index I. The values $u^{(j)}$ are determined by (I.11) and (I.12), and for amplitudes $D_0^{(j)}$ and $D_h^{(j)}$ one has the following relation:

$$D_h^{(j)} = \frac{u^{(j)2} - \varphi_0^2 - \chi_0}{\chi_h} D_0^{(j)}. \quad (7)$$

To determine the amplitudes E_0^s and E_h^s one has to use the continuity conditions of the wave fields and their derivatives both at the boundary vacuum–amorphous film and at the amorphous film–crystal surface interface.

As a result we have the following eight equations:

$$\begin{aligned} E_0 + E_0^s &= \mathcal{E}_0 + \mathcal{E}_0^s, & E_h^s &= \mathcal{E}_h + \mathcal{E}_h^s, \\ \varphi_0(E_0 - E_0^s) &= y_0^{\text{am}}(\mathcal{E}_0 - \mathcal{E}_0^s), & -\varphi_h E_h^s &= y_h^{\text{am}}(\mathcal{E}_h - \mathcal{E}_h^s), \end{aligned} \quad (8)$$

at the vacuum–amorphous film interface;

$$\begin{aligned} \mathcal{E}_j e^{id_j} + \mathcal{E}_j^s e^{-id_j} &= D_j^{(1)} + D_j^{(2)}, \\ y_j^{\text{am}}(\mathcal{E}_j e^{id_j} - \mathcal{E}_j^s e^{-id_j}) &= u^{(1)}D_j^{(1)} + u^{(2)}D_j^{(2)}; \end{aligned} \quad j = 0, h \quad (8')$$

at the amorphous film–crystal surface interface.

Here

$$d_{0,h} = \boldsymbol{\kappa} t y_{0,h}^{\text{am}}. \quad (9)$$

Accounting the two equations (7) one has a set of ten equations, just enough to determine ten unknown amplitudes: E_0^s , E_h^s , \mathcal{E}_0 , \mathcal{E}_0^s , \mathcal{E}_h , \mathcal{E}_h^s , $D_0^{(1)}$, $D_0^{(2)}$, $D_h^{(1)}$, $D_h^{(2)}$.

Since the set is linear, its solution can be found directly. We are interested only in the reflected-diffracted wave amplitude E_h^s . Omitting intermediate transformations we give the final expression

$$E_h^s = \frac{-2\varphi_0 \chi_h (u^{(2)} - u^{(1)})}{W^{(2)} b_0^{(2)} b_h^{(1)} - W^{(1)} b_0^{(1)} b_h^{(2)}} E_0, \quad (10)$$

where

$$b_{0,h}^{(1)} = \frac{1}{2} \left[\left(1 - \frac{\varphi_{0,h}}{y_{0,h}^{\text{am}}} \right) (u^{(2)} - y_{0,h}^{\text{am}}) e^{id_{0,h}} + \left(1 + \frac{\varphi_{0,h}}{y_{0,h}^{\text{am}}} \right) (u^{(2)} + y_{0,h}^{\text{am}}) e^{-id_{0,h}} \right], \quad (11)$$

$b_{0,h}^{(2)}$ being defined by the same formula as (11) with substituting index 2 for 1 and vice versa. The other values were determined in [3],

$$W^{(1,2)} = -\frac{\alpha}{2} \pm \sqrt{\left(\frac{\alpha}{2}\right)^2 + \chi_h \chi_h^-}, \quad (12)$$

$$u^{(1,2)} = \pm \sqrt{\varphi_0^2 + \chi_0 + W^{(1,2)}}. \quad (13)$$

The sign of the root in (13) is determined from the condition

$$\text{Im } u^{(j)} > 0. \quad (14)$$

Equations (10) to (14) provide a complete solution of the problem under consideration.

The reflected-diffracted wave intensity should be naturally determined by the coefficient

$$P_h^s = \frac{\varphi_h}{\varphi_0} \left| \frac{E_h^s}{E_0} \right|^2. \quad (15)$$

It can be easily seen that for $t = 0$ (15) reduces to the equation for P_h^s obtained in [3] for ideal crystals.

3. The Effect of an Amorphous Film

The presence of an amorphous film first of all results in additional specular reflection of both incident wave and reflected-diffracted wave formed in the crystal. Both these factors are revealed as a decrease in the reflected-diffracted intensity. Mathematically the film effect is displayed through the factors $e^{\pm id_{0,h}}$ in (11). Naturally, the distortion of the diffraction pattern begins when

$$d_{0,h} \geq 1. \quad (16)$$

From (16) already the depth scale follows at which the amorphous film effect begins to be revealed,

$$t \geq t_c \left| \sqrt{\frac{\chi_0^{\text{am}}}{\varphi_{0,h}^2 + \chi_0^{\text{am}}}} \right|, \quad (17)$$

where

$$t_c = \frac{\lambda}{2\pi |\chi_0^{\text{am}}|}. \quad (18)$$

For example, for CuK_α radiation ($\lambda = 0.154$ nm) t_c is of the same order for silicon film (≈ 5 nm) and for Ge film (≈ 3 nm).

Fig. 2a shows the curves $P_h^s(\varphi_h)$ for films of various depth. Calculations were performed for a silicon crystal, 220 reflection, CuK_α radiation. The incident angle was chosen to be less than the critical angle for total external reflection. It was assumed that $\chi_0^{\text{am}} = \chi_0$, for the sake of simplicity. As can be seen from Fig. 2a, a film of 1 nm depth causes an intensity attenuation by $\approx 25\%$.

So in this case one deals with a unique sensitivity of X-ray diffractometry to very thin amorphous films on crystal surfaces.

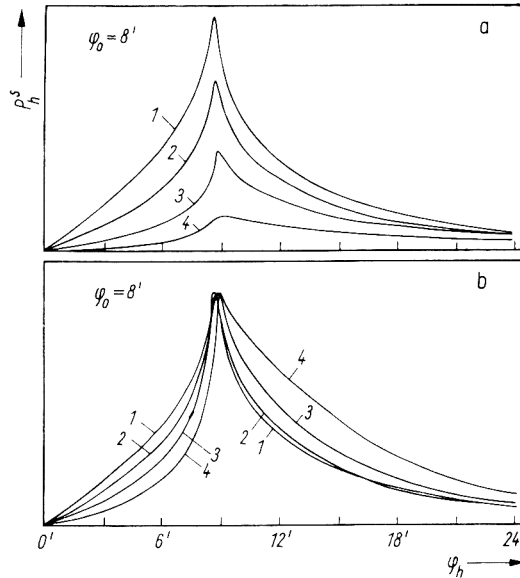


Fig. 2. The plots of the specularly reflected-diffracted intensity vs. φ_h for small incident angle value ($\varphi_0 < \varphi_c \equiv \sqrt{|\chi_0|}$) and films with $t \approx 1$ to 5 nm. Si, $\text{CuK}\alpha$ radiation, 220 reflection, $\varphi_c = 13.34'$. (1) Crystal without film ($t = 0$), (2) $t = 1$, (3) 2.5, (4) 5 nm. a) In absolute units; b) in relative units

The presence of an amorphous film is revealed not only as an absolute drop of reflected-diffracted intensity, but also in the deformation of the curve shape. All curves on Fig. 2b were reduced to the same scale. As can be seen from this figure, even in such a case it is possible to determine precisely films of thickness $t \approx 2.5$ nm.

To determine film thicknesses $t \leq 5$ nm it is convenient to carry out measurements at small values of the incident angle ($\varphi_0 < \sqrt{|\chi_0|}$). However, for thicker films it is expedient for maintaining the intensity to choose greater values of the incident angle ($\varphi_0 > \sqrt{|\chi_0|}$). Fig. 3 shows a plot of exponential damping depth of the X-ray intensity in an amorphous film versus the variation of the incident angle, as given by the formula

$$l_0 = \frac{\lambda}{2\pi \text{Im} \sqrt{\varphi_0^2 + \chi_0^{\text{am}}}} \quad (19)$$

Outside the total external reflection range the damping of the incident wave intensity in an amorphous film decreases sharply, and the intensity is maintained for films with a thickness as large as ≈ 200 nm.

In this angular range the amorphous film effect is displayed through the intensity damping of the diffracted wave emerging out of the crystal and through a variation of the phase relations between the wave fields. The damping of the reflected diffracted

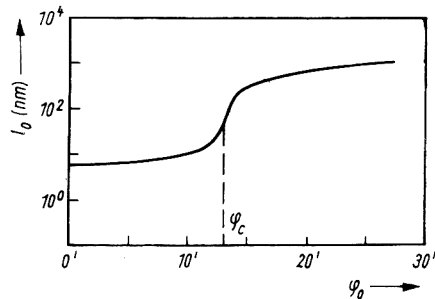


Fig. 3. The plot of X-ray exponential damping depth in amorphous film vs. incident angle value

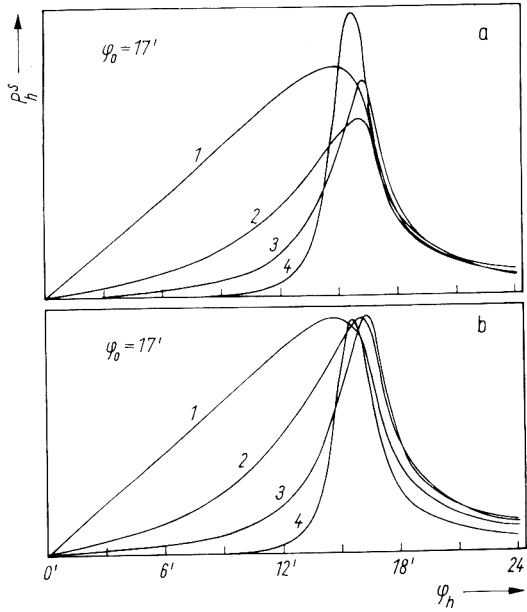


Fig. 4

Fig. 4. The plots of the specularly reflected-diffracted intensity vs. φ_h for large incident angle value ($\varphi_0 > \varphi_c$). The intensity attenuation at small exit angles for films with $t \approx 5$ to 20 nm. (1) Crystal without film ($t = 0$), (2) $t = 5$, (3) 10, (4) 20 nm. a) In absolute units; b) in relative units

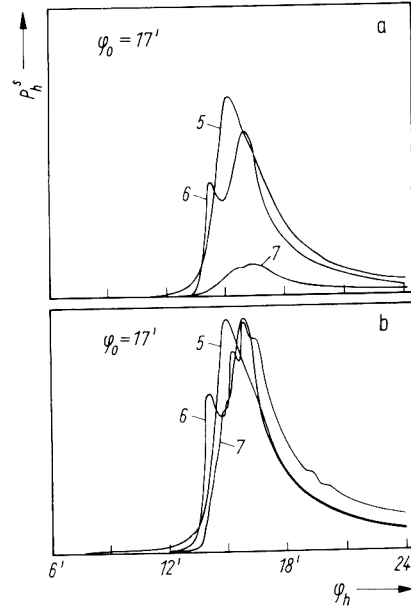


Fig. 5

Fig. 5. The plots of the specularly reflected-diffracted intensity vs. φ_h for large incident angle value ($\varphi_0 > \varphi_c$). Oscillations on the curves for films with $t \approx 20$ to 200 nm. (5) $t = 30$, (6) 50, (7) 200 nm. a) In absolute units; b) in relative units

intensity in an amorphous film can be described approximately by the factor

$$f = e^{-t/l_h}, \quad (20)$$

where l_h is defined by (19) with substituting the index "h" instead of "h'". A strong attenuation of the intensity takes place in the range of exit angles $\varphi_h < \sqrt{|\chi_0|}$. It gives the possibility to reveal films with depth of the order of ≈ 5 to 20 nm through an intensity decreasing (see Fig. 4).

For films with a thickness $t \approx 20$ to 200 nm the main differences are caused by variations of the phase relations between wave fields and this fact leads to the appearance of oscillations (see Fig. 5). The presence of these oscillations provides the possibility to draw conclusions as to the film homogeneity, and, on the other hand, it is possible to determine the thickness of the film from the angular interval between intensity maxima (minima) of the curve.

It is to be noted that the term "amorphous film" means not only a film of amorphous material here, but it may also be a crystalline film in which the diffraction conditions are not satisfied. For instance, it may be a crystalline surface layer in which an abnormal content of defect clusters causes a relative change of the lattice spacing of the same order as $\approx 10^{-4}$.

Acknowledgement

The authors would like to express their thanks to Dr. R. M. Imamov for his encouragement and useful discussions.

References

- [1] W. C. MARRA, P. EISENBERGER, and A. Y. CHO, *J. appl. Phys.* **50**, 6927 (1979).
- [2] P. EISENBERGER and W. C. MARRA, *Phys. Rev. Letters* **46**, 1081 (1981).
- [3] A. M. AFANASIEV and M. K. MELKONYAN, *Acta cryst.* **A39**, 207 (1983).
- [4] P. FARWIG and H. W. SCHURMANN, *Z. Phys.* **204**, 489 (1967).
- [5] T. BEDYŇSKÁ, *phys. stat. sol. (a)* **25**, 405 (1974).
- [6] V. C. BARYSHEVSKII, *Zh. tekhn. Fiz., Pisma* **2**, 112 (1976).
- [7] A. L. GOLOVIN, R. M. IMAMOV, and S. A. STEPANOV, *Acta cryst.*, in the press.

(Received July 5, 1983)